

The design and preparation of metabolically protected new arylpiperazine 5-HT_{1A} ligands

Manish Tandon, Mary-Margaret O'Donnell, Alex Porte, David Vensel, Donglai Yang, Rocio Palma, Alan Beresford and Mark A. Ashwell*

ArQule Inc., 19 Presidential Way, Woburn, MA 01801, USA

Received 8 December 2003; revised 16 January 2004; accepted 19 January 2004

Abstract—New arylpiperazines related to buspirone, gepirone and NAN-190 were designed and screened in silico for their 5-HT_{1A} affinity and potential sites of metabolism by human cytochrome P450 (CYP3A4). Modifications to these structures were assessed in silico for their influence on both 5HT_{1A} affinity and metabolism. Selected new molecules were synthesized and purified in a parallel chemistry approach to determine structure activity relationships (SARs). The resulting molecules were assessed in vitro for their 5HT_{1A} affinity and half-life in a heterologously expressed human CYP3A4 assay. Molecular features responsible for 5-HT_{1A} affinity and CYP3A4 stability are described.

© 2004 Elsevier Ltd. All rights reserved.

The cytochrome P450 3A4 (CYP3A4) has a broad range of substrate specificity and is responsible for metabolizing nearly 50% of marketed drugs.¹ It is therefore a significant challenge in the pursuit of orally active small molecule therapeutics. Due to CYP3A4s broad substrate specificity, predicting which site on a drug is susceptible to metabolism by this enzyme has proved difficult. We initiated a library design project incorporating our predictive global site lability CYP3A4 model to aid in the identification of new 5-HT_{1A} ligands with increased stability towards CYP3A4 metabolism. Buspirone, **1**² is a known drug, which is metabolized in vivo primarily by CYP3A4. Therefore it was selected as the structural manifold on which to demonstrate a parallel design and synthesis process.

Our objective was 3-fold; (a) maintain or improve in vitro 5HT_{1A} affinity compared to **1** (Table 1, IC₅₀ = 25 nM, upper limit for new designs = 250 nM), (b) increase the stability to CYP3A4 metabolism 2-fold or greater compared to **1** (Table 1, t_{1/2} = 4.6 min) and (c) to provide additional SAR data to refine our predictive models to further increase their effectiveness in designing additional molecules with improved 5HT_{1A} activity and CYP3A4 stability. Herein we report the results of our

initial findings for (a) and (b) and provide a summary of the SAR. We discuss the structural changes made in relationship to the measured 5-HT_{1A} affinity and CYP 3A4 stability.

The CYP3A4 metabolism model estimates regioselectivity by calculating the relative stabilities of free radicals using semi-empirical quantum calculations.³ The model is generally applicable as it is not derived from limited structure–activity information and requires only a structure as input. The resulting free energy estimates are combined with steric accessibility and global orientation terms to rank-order regiolabilities. The total susceptibility to metabolism is categorized relative to the competing decoupling reaction resulting in the formation of water: sites that have predicted rates of metabolism much greater than that of water formation are classed as highly labile, while those that have much lower rates are classed as stable.

Although the number of predicted labile sites in a molecule may not correlate directly to the rate of metabolism, the relative number of labile sites in a molecule corresponds to the number of modifications required to improve its stability.

The visual representation of the metabolic landscape (Fig. 1) assigns the different sites of metabolism as labile, moderately labile, moderately stable and stable.

* Corresponding author. Tel.: +1-781-994-0598; fax: +1-781-994-0690; e-mail: mashwell@arqule.com

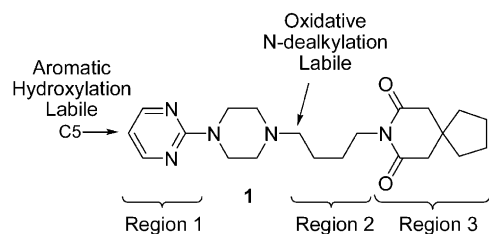


Figure 1. Metabolic landscape of buspirane **1** as predicted by CYP3A4 model (most labile sites shown).

Furthermore this analysis provides relative proportions of each metabolite likely to be formed by CYP3A4.

The predicted metabolic landscape for **1** (Fig. 1, only labile sites depicted) is in good agreement with the reported experimental data.⁴ Specifically, it shows a propensity (labile) for aromatic hydroxylation at C5 of the pyrimidine ring and oxidation on the carbon *alpha* to the piperazine ring (labile), which leads to N-dealkylation producing 1-pyrimidinyl-piperazine. Both of these sites are metabolized *in vivo*. Our design strategy assumed that a reduction in the number of labile sites in the molecule would result in concomitant increase in the stability towards the CYP3A4.

Our synthetic strategy was devised to provide straightforward access to molecules modified at the primary sites of metabolism. The most labile sites were addressed first as these were expected to have the most dramatic effect on the overall stability of the molecule.

The scaffold was divided into three regions (Fig. 1) and new compounds were designed around these. The protonatable arylpiperazine recognition element, crucial for 5-HT_{1A} affinity, was maintained in all designs.⁵

Substituents R₁, R₂ and R₃, in Region 2 were filtered to reject any combination which (a) rendered the basic N on the arylpiperazine non-basic, as predicted by ACD pK_a predictor⁶ and (b) did not fit the Catalyst pharmacophore model. This pharmacophore was constructed from literature data and was consistent with the established SAR requiring the presence of a basic arylpiperazine nitrogen, an aromatic hydrophobe and a hydrogen bond acceptor. The pharmacophore preferred an extended conformation in agreement with published CoMFA models.⁷ The pharmacophore provided a powerful and convenient predictive tool with which to apply the known SAR.

In an iterative virtual design process, structural modifications in each region were made and the effect on predicted CYP3A4 was assessed. If the design was accepted the two remaining regions were also subjected to virtual library enumeration. The prioritized virtual arrays were then assessed in both the CYP3A4 and the 5-HT_{1A} models. A similar process was employed to address multiple sites in parallel.

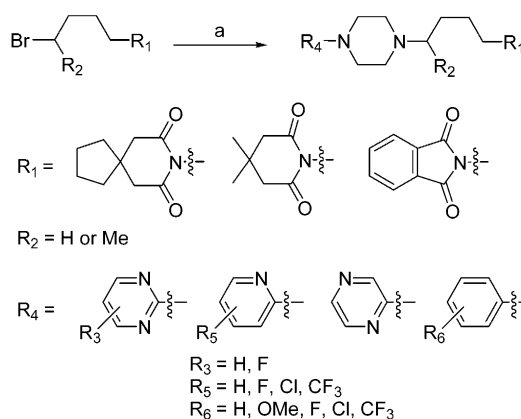
The labile site of Region 1 was addressed by; (1) blocking the oxidation site with a fluorine atom, (2) replacing the pyrimidine ring with either a 2-pyridine or 2-pyra-

zine or with substituted phenyl rings. The labile site in Region 2 was addressed by incorporation of (1) a steric block (alpha methyl or beta *gem* dimethyl), (2) an electronic block with a beta OH, (3) a combination of a methyl group and OH on the beta carbon. The study was extended to include two additional Region 3 variants, the 4,4-dimethylpiperidinone of gepirone and the phthalimide of NAN-190 with both straight chain and alpha methyl variants.⁸

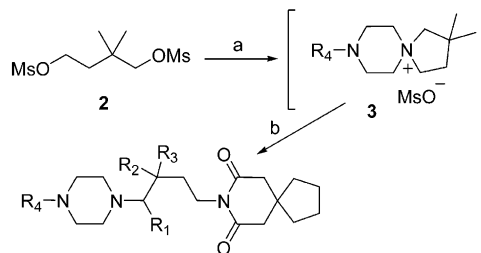
All straight chain and alpha methyl analogues were prepared as shown in Scheme 1.⁹

Focused libraries containing only the 3,3-tetramethyleneglutarimide in Region 3 were prepared by reacting aryl piperazines with the dimesylate of 2,2-dimethylbutane-1,4-diol **2** to give the cyclic quarternary ammonium salts **3**. Which upon treatment with 3,3-tetramethyleneglutarimide gave the final products as shown in Scheme 2.¹⁰

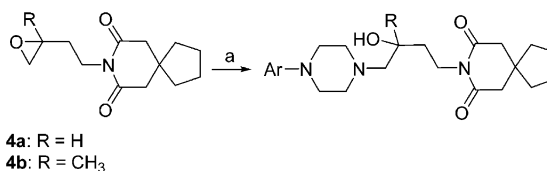
Access to the analogues modified with both a methyl and a hydroxyl group on the *beta* carbon was achieved by reacting the epoxides **4** with aryl piperazines as described in Scheme 3.



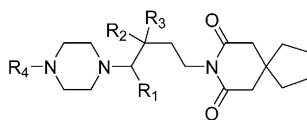
Scheme 1. (a) Aryl piperazine, K₂CO₃, DMF, 80 °C.



Scheme 2. (a) Aryl piperazines, DMF, decant.; (b) 3,3-tetramethyleneglutarimide, K₂CO₃, DMF, 100 °C.



Scheme 3. (a) Aryl piperazine, LiClO₄, CH₃CN, 80 °C.

Table 1. Region 1 and 2 SAR of the 3,3-tetramethyleneglutarimide containing analogues

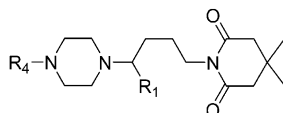
Compd	R ₁	R ₂	R ₃	R ₄	5-HT _{1A} IC ₅₀ (μM) ^a	CYP 3A4 t _{1/2} (min) ^b
1	H	H	H	Pyrimidine	0.025	4.6
5	H	H	H	5-F Pyrimidine	0.063	52.3
6	H	H	H	<i>p</i> -F phenyl	0.064	3.2
7	H	H	H	2-Pyrazine	0.46	5.5
8	H	H	H	<i>p</i> -OMe Phenyl	0.93	21.1
9	Me	H	H	Pyrimidine	0.004	3.8
10	Me	H	H	5-F Pyrimidine	0.046	14.8
11	H	Me	Me	Pyrimidine	0.71	2.9
12	H	H	H	<i>o</i> -OMe Phenyl	0.002	5.1
13	H	OH	H	Pyrimidine	0.84	10.2
14	H	OH	Me	Pyrimidine	1.46	8.6
15	H	OH	H	2-Pyrazine	> 1.0	9.6
16	H	OH	H	<i>o</i> -OMe Phenyl	0.012	7.8
17	H	OH	H	<i>p</i> -F phenyl	0.069	3.8
18	Me	H	H	<i>p</i> -F phenyl	0.099	2.4
19	H	H	H	Phenyl	0.015	8.0

^a Binding affinity at 5-HT_{1A} receptors labeled with [³H]-8-OH-DPAT.

^b LC/MS/MS analysis of parent ion fragmentation at each time point, peak area reported normalized to internal standard.

Analysis of modifications in Region 1 (Region 2 and 3 fixed as in **1**) demonstrates that the labile site (5-position in pyrimidine ring) plays a dominant role in determining overall stability to CYP 3A4 metabolism¹¹ (Table 1).

When the C5 position is substituted with a fluorine atom as in **5**, 5-HT_{1A} affinity¹² is maintained (63 nM) and the compound is more stable than **1**. However, when the Region 2 labile site is blocked with a methyl group as in **9** (or a beta *gem* dimethyl **11**), the stability is not improved compared to **1**. Removal of both labile sites by introduction of an alpha methyl into **5** providing **10** decreases CYP3A4 stability relative to **5**. Our global CYP3A4 model did not accurately predict this. In general, introduction of a methyl group alpha to the piperazine ring reduces CYP3A4 stability compared to the unsubstituted analogues a trend, which held true when the Region 3 substituent was varied (compare **20** and **21** and **23** and **24** in Tables 2 and 3).

Table 2. Region 1 SAR of the 4,4-dimethylpiperidine-2,6-dione analogues

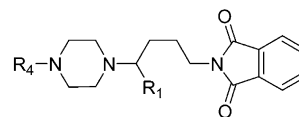
Compd	R ₁	R ₄	5-HT _{1A} IC ₅₀ (μM) ^a	CYP 3A4 t _{1/2} (min) ^b
20	H	Pyrimidine	0.114	30.3
21	H	5-F Pyrimidine	0.205	78.3
22	Me	5-F Pyrimidine	0.087	40.1

^a Binding affinity at 5-HT_{1A} receptors labeled with [³H]-8-OH-DPAT.

^b LC/MS/MS analysis of parent ion fragmentation at each time point, peak area reported normalized to internal standard.

Removal of the Region 2 labile site by introduction of beta-OH was successful in providing analogues with increased metabolic stability. For example analogue **13** had improved stability (t_{1/2} = 10.2 min) with respect to **1** (t_{1/2} = 4.6 min). The same trend is observed with the regioisomeric **15** and its unsubstituted parent **7**. However, both **13** and **15** are considerably less potent 5-HT_{1A} ligands than **1**. No additional improvement either in stability or affinity is seen when both a methyl and a -OH are combined on the same carbon atom of **1**, as in **14**.

Significantly, the introduction of a beta -OH group in Region 2 did not reduce the 5-HT_{1A} affinity as dramatically when introduced into the 2-OMePh substituted piperazines (common to many potent 5-HT_{1A} ligands). A comparison of the unsubstituted **12** and its beta-OH analogue **16** shows that the more metabolically stable **16** also has good 5-HT_{1A} affinity.

Table 3. Region 1 SAR of the phthalimide containing analogues

Compd	R ₁	R ₄	5-HT _{1A} IC ₅₀ (μM) ^a	CYP 3A4 t _{1/2} (min) ^b
23	H	Pyrimidine	0.06	26.8
24	H	5-F Pyrimidine	0.44	20.4
25	Me	5-F Pyrimidine	0.21	18.2

^a Binding affinity at 5-HT_{1A} receptors labeled with [³H]-8-OH-DPAT.

^b LC/MS/MS analysis of parent ion fragmentation at each time point, peak area reported normalized to internal standard.

Introduction of either a F or OMe block on to the 4 position of the arylpiperazine again highlights the difficulty in maintaining 5-HT_{1A} affinity while increasing metabolic stability. Although the 4-fluorophenyl analogues (**6**, **17** and **18**) are all potent, none of them have improved stability relative to **1** or the unsubstituted phenyl, **19**. In contrast, the alternate blocking substituent 4-OMe of **8**, while increasing metabolic stability, reduces activity to the unacceptable micromolar level.

We were predominantly interested in modifications to reduce CYP3A4 metabolism at those sites indicated to be most labile by our predictive model. However, we also wanted to explore the role of the substituent in Region 3. It has recently been suggested that a general strategy for avoiding CYP2D6 metabolism in compounds related to **1**, is to introduce bulky substituents into Region 3.¹³

Our findings from this study demonstrate that these bulky substituents also dramatically affect the metabolism by CYP3A4. Overall stability is greatest when Region 3 contains 4,4-dimethylpiperidinone, followed by phthalimide (Table 2) and is least with 3,3-tetramethyleneglutarimide (Table 3), as in **1**.

A design-make-test paradigm was implemented to assess the impact of an in silico model of human CYP3A4 metabolism. We successfully demonstrated the use of in silico models for 5-HT_{1A} affinity and CYP3A4 metabolism. Strategies were found which maintained 5-HT_{1A} affinity and improved in vitro CYP3A4 stability within the limits established for the goals of the project. Key SAR features which emerged were: (i) the effect of steric crowding around the site of N-dealkylation negatively affecting the CYP3A4 stability, (ii) introduction of a hydroxyl group beta to this site which increased metabolic stability and (iii) the previously under appreciated effect of the Region 3 substituent in determining the rate of CYP3A4 metabolism for this general class of arylpiperazine 5HT_{1A} ligands.

In general, for close structural analogues of **1** significant improvements in stability against CYP3A4 were always at the expense of 5-HT_{1A} affinity except in the case of the known incorporation of a 5-F substituent into the pyrimidine ring. Other potent 5-HT_{1A} arylpiperazine templates such as 2-OMePh had improved CYP3A4 stability and maintained affinity when substituted with a beta OH.

This work and additional analogues provided invaluable SAR for the construction and implementation of a new local CYP3A4 rate model design, which will be described in detail elsewhere.

Acknowledgements

We thank Drs. Ken Korzekwa and Stuart Russell for their pADME modeling insight, Dr. Andrew Smellie for his molecular modeling assistance and Dr. Sheila DeWitt and Dr. Valery Antonenko for their support of this project.

References and notes

1. Rendic, S. *Drug Metab. Rev.* **2002**, *34*, 83.
2. (a) Wu, Y.-H.; Rayburn, J. W.; Allen, L. E.; Ferguson, H. C.; Kissel, J. W. *J. Med. Chem.* **1972**, *15*, 477. (b) Tunicliff, G.; Eison, A. S.; Taylor, D. P., Eds. In *Buspirone: Mechanism and Clinical Aspects*; Academic Press Inc, 1991.
3. (a) Jones, J. P.; Mysinger, M.; Korzekwa, K. R. *Drug Metab. Dispos.* **2002**, *30*, 7. (b) Korzekwa, K. R.; Jones, J. P.; Gillette, J. R. *J. Am. Chem. Soc.* **1990**, *112*, 7042.
4. (a) Jajoo, H. K.; Mayol, R. F.; LaBudde, J. A.; Blair, I. A. *Drug Metab. Dispos.* **1989**, *17*, 634. (b) Jajoo, H. K.; Mayol, R. F.; LaBudde, J. A.; Blair, I. A. *Drug Metab. Dispos.* **1989**, *17*, 625. (c) Sakr, A.; Andheria, M. *J. Clin. Pharmacol.* **2001**, *41*, 886.
5. Lopez-Rodriguez, M. L.; Ayala, D.; Benhamu, B.; Morcillo, M. J.; Viso, A. *Curr. Med. Chem.* **2002**, *9*, 443.
6. PhysChem Batch software, v6.13; http://www.acdlabs.com/products/phys_chem_lab/pka/
7. Lopez-Rodriguez, M. L.; Rosado, M. L.; Benhamu, B.; Morcillo, M. J.; Fernandez, E.; Schaper, K.-J. *J. Med. Chem.* **1997**, *40*, 1648.
8. Glennon, R. A.; Naiman, N. A.; Pierson, M. E.; Titeler, M.; Lyon, R. A.; Herndon, J. L.; Misenheimer, B. *Drug Dev. Res.* **1989**, *16*, 335.
9. All new compounds were prepared in a parallel chemistry fashion, purified by RP-HPLC and characterized by HPLC-MS.
10. Ishizumi, K.; Kojima, A.; Antoku, F.; Ikutaro, S.; Yoshigi, M. *Chem. Pharm. Bull.* **1995**, *43*, 2139.
11. For a detailed description of the assay methodology see: Saraswat, L.; Caserta, K. A.; Laws, K.; Wei, D.; Jones, S. J.; Adedoyin, A. *J. Biomolecular Screening* **2003**, *8*, 544.
12. The method was based on a scintillation proximity assay previously described but adapted for human 5-HT_{1A} binding: Kahl, S. D.; Hubbard, F. R.; Sittampalam, G.; Zock, J. M. *J. Biomolecular Screening* **1997**, *2*, 33.
13. Kalgutkar, A. S.; Zhou, S.; Fahmi, O. A.; Taylor, T. J. *Drug Metab. Dispos.* **2003**, *31*, 596.